Macromolecules
ARTICLE

Macromolecules **2009**, *42*, 5007–5016 **5007**
DOI: 10.1021/ma900788k

Click Coupling Fullerene onto Thermoresponsive Water-Soluble Diblock Copolymer and Homopolymer Chains at Defined Positions

Changhua Li, Jinming Hu, Jun Yin, and Shiyong Liu*

CAS Key Laboratory of Soft Matter Chemistry, Department of Polymer Science and Engineering, Hefei National Laboratory for Physical Sciences at the Microscale, University of Science and Technology of China, Hefei, Anhui 230026, China

Received April 10, 2009; Revised Manuscript Received May 5, 2009

ABSTRACT: We report on the synthesis of well-defined thermoresponsive water-soluble diblock copolymer and homopolymers functionalized with controlled numbers of C_{60} moieties at predetermined positions via the combination of atom transfer radical polymerization (ATRP) and click chemistry. Azide-containing polymer precursors including monoazide-terminated and α,α-diazide-terminated poly(*N*-isopropylacrylamide), N_3- PNIPAM and $(N_3)_2$-PNIPAM, as well as poly(ethylene glycol)-*b*-PNIPAM with one azide moiety at the diblock junction, PEG(-N_3)-*b*-PNIPAM, were synthesized via ATRP using specific azide-functionalized small molecule and polymeric initiators. On the other hand, the reaction of 4-prop-2-ynyloxybenzaldehyde with pristine C_{60} in the presence of glycine afforded alkynyl-modified C_{60}, *alkynyl*-C_{60}. Subsequently, the click reaction of N_3-PNIPAM, $(N_3)_2$-PNIPAM, and PEG(-N_3)-*b*-PNIPAM led to the facile preparation of thermoresponsive diblock copolymer and homopolymers functionalized with controlled numbers of C_{60} at designed positions, including C_{60}-PNIPAM, $(C_{60})_2$-PNIPAM, and PEG(-C_{60})-*b*-PNIPAM. All the intermediate and final products were characterized by ^{1}H NMR, Fourier transform infrared spectroscopy (FT-IR), UV−vis spectroscopy, thermogravimetric analysis (TGA), and gel permeation chromatograph (GPC) equipped with UV/RI dual detectors. C_{60}-containing hybrid nanoparticles were then fabricated via supramolecular self-assembly of C_{60}-PNIPAM, $(C_{60})_2$-PNIPAM, and PEG(-C_{60})-*b*-PNIPAM in aqueous solution, which were characterized by dynamic and static laser light scattering (LLS) and transmission electron microscopy (TEM). These novel fullerenated polymers retain the thermoresponsiveness of PNIPAM-based precursors, and self-assembled hybrid nanoparticles exhibit thermo-induced collapse/aggregation behavior due to the lower critical solution temperature (LCST) phase transition of PNIPAM chains.

Introduction

As a representative member of the fullerene family, C_{60} has attracted ever-increasing attention since the discovery that fullerene-containing materials possess unique physical and chemical properties, which endow them with promising applications in superconductors, ferromagnets, lubrications, photoconductors, catalysts, and molecular medicines.[1,2] However, the poor solubility of fullerenes, especially in water, considerably limits their practical applications.[3] Therefore, they have to be covalently or noncovalently modified to improve the water solubility. Several strategies have been explored to enhance the solubility of fullerenes in water.[4−18] For example, water-soluble fullerene carboxylic acid derivatives, fullerenols, fullerene amino acids, and the corresponding supramolecular derivatives were prepared and investigated in terms of their biochemical and medicinal activities.[4−9] In particular, the introduction of C_{60} into water-soluble polymers has been recognized as one of the simplest strategies to enhance its solubility in water, while retaining the unique properties of C_{60}.[10−18] Moreover, the presence of polymeric species adds extra functionality and versatility in designing C_{60}-based functional materials.[19,20]

A variety of approaches have been developed for the synthesis of C_{60}-contianing hybrid polymers.[11,15−18,21−39] Among them, the thermal [3 + 2] cycloaddition reaction between azido-functionalized polymers and pristine C_{60} has been frequently employed,[21−29] as originated by Hawker and co-workers.[21] Later on, Tam et al.[16−18] and Goh et al.[22−24] also reported several excellent examples in this aspect. Despite its high efficiency, it is still challenging to eliminate multiple addition products during cycloaddition reaction of pristine C_{60} with azide moieties. Very recently, Cheng et al.[40] reported a novel approach for the synthesis of C_{60}-containing hybrid polymers via click reaction[41−44] of monoazide-terminated polystyrene (PS) and alkynyl-functionalized C_{60}. They successfully proved that this strategy provides a highly efficient and quantitative reaction for the formation of stable and well-defined fullerenated materials under quite mild reaction conditions.

PNIPAM homopolymer dissolves in cold and dilute aqueous solution but becomes insoluble at ~32 °C due to its lower critical solution temperature (LCST) phase transition behavior.[45−52] Recently, Geckeler et al.[37] and Yajima et al.[29] investigated the aggregation behavior of poly(*N*-isopropylacrylamide) (PNIPAM) functionalized with one C_{60} moiety (C_{60}-PNIPAM) in aqueous solution. The presence of highly hydrophobic C_{60} leads to intriguing self-assembling behavior when it is incorporated into thermoresponsive PNIPAM chains at the chain terminal. In the above two examples, the addition reaction between C_{60} and macromolecular PNIPAM radicals generated under reversible addition−fragmentation chain-transfer (RAFT) conditions as well as the thermal [3 + 2] cycloaddition reaction between azido-terminated PNIPAM and C_{60} were employed in the synthesis of C_{60}-terminated PNIPAM, respectively. To further control the nanostructures of self-assembled aggregates from

*To whom correspondence should be addressed. E-mail: sliu@ustc.edu.cn.

Published on Web 05/21/2009

Scheme 1. Synthetic Routes for the Preparation of *Alkynyl-C_{60}* Precursor

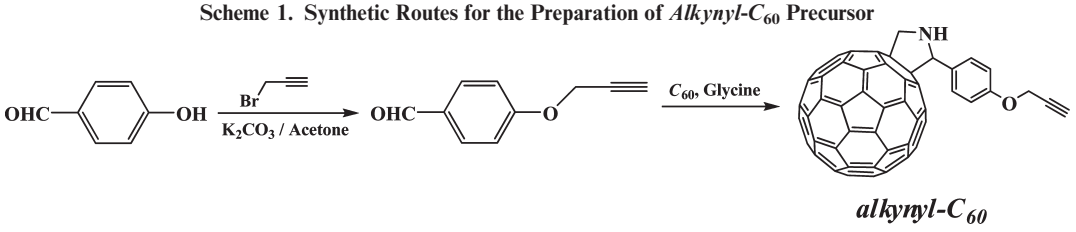

Scheme 2. Synthetic Routes Employed for the Preparation of (a) C_{60}-PNIPAM$_{98}$, (b) $(C_{60})_2$-PNIPAM$_{100}$, and (c) PEG$_{113}$(-C_{60})-*b*-PNIPAM$_{70}$

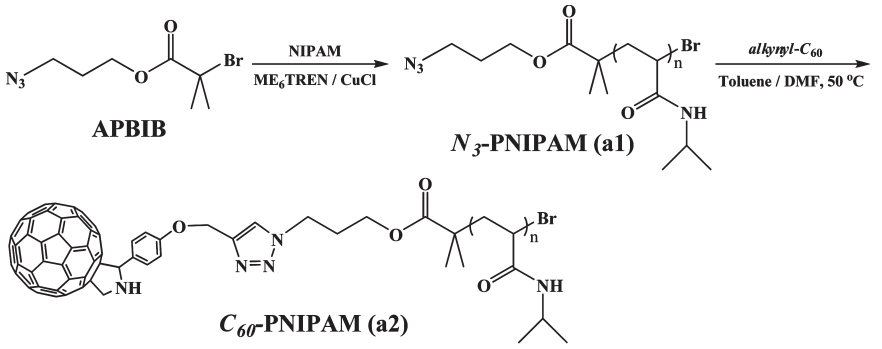

(*a*)

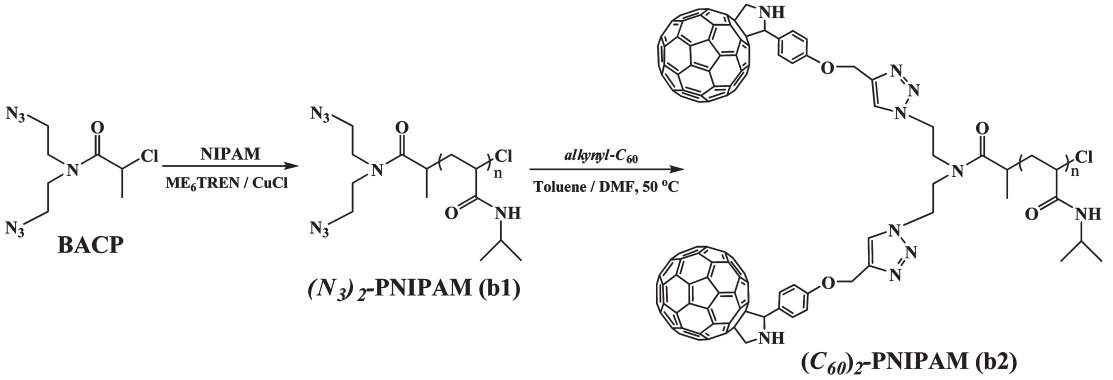

(*b*)

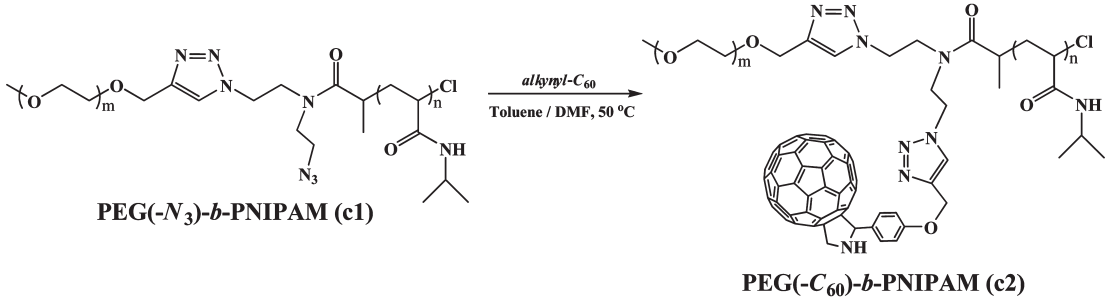

(*c*)

fullerenated polymers and maintain their colloidal stability in aqueous media, it is highly desirable to synthesize C_{60}-containing water-soluble polymers with more complex chain architectures, tunable functionalities, and suitable stimuli responsiveness.

In this work, we report on the synthesis of well-defined thermoresponsive PNIPAM-based diblock copolymer and homopolymers embedded with controlled numbers of C_{60} functionality at predetermined positions via the combination of atom transfer radical polymerization (ATRP) and click chemistry. Alkynyl-modified C_{60}, *alkynyl-C_{60}*, and azide-containing polymer precursors were synthesized at first (Schemes 1 and 2). Next, the click reaction of *alkynyl-C_{60}* with monoazide-terminated and α,α-diazide-terminated poly(*N*-isopropylacrylamide), N_3-PNIPAM and $(N_3)_2$-PNIPAM, as well as poly(ethylene glycol)-*b*-PNIPAM with one azide moiety at the diblock junction, PEG(-N_3)-*b*-PNIPAM, afforded water-soluble diblock copolymer and homopolymers embedded with controlled numbers of C_{60} at designed positions, including C_{60}-PNIPAM, $(C_{60})_2$-PNIPAM, and PEG(-C_{60})-*b*-PNIPAM (Schemes 2 and 3). We further investigated their supramolecular self-assembly as well as thermoresponsive collapse/aggregation behavior in aqueous solution by employing dynamic and static laser light scattering (LLS),

Scheme 3. Schematic Illustration of the Synthesis of Thermoresponsive Diblock Copolymer and Homopolymers Embedded with C_{60} at Predetermined Position via Click Reaction of *Alkynyl-C_{60}* with Well-Defined Azido-Containing Precursors

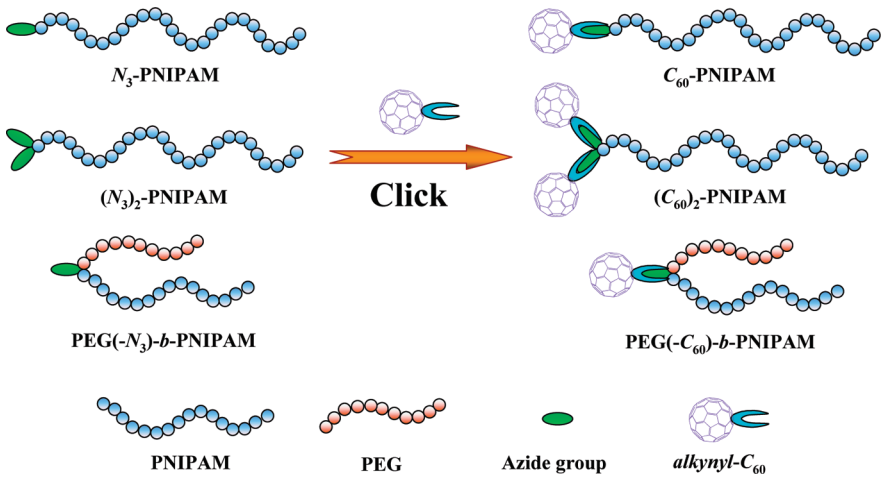

temperature-dependent optical transmittance, and transmission electron microscopy (TEM).

Experimental Section

Materials. *N*-Isopropylacrylamide (NIPAM) (97%, Tokyo Kasei Kagyo Co.) was purified by recrystallization from a mixture of benzene and *n*-hexane (1/3, v/v). Poly(ethylene glycol) monomethyl ether (PEG_{113}-OH, M_n = 5000, M_w/M_n = 1.06, mean degree of polymerization, DP, is 113), C_{60} (99.5%), 2-chloropropionyl chloride (97%), and *N*,*N*,*N*′,*N*″,*N*″-pentamethyldiethylenetriamine (PMDETA, 99%) were purchased from Aldrich and used as received. Tris(2-aminoethyl)amine (TREN), bis(2-chloroethyl)amine hydrochloride (98%), copper(I) chloride (CuCl, 99.99%), and 2-bromoisobutyryl bromide (97%) were purchased from Fluka and used as received. Sodium azide (NaN_3, 99%), propargyl alcohol, and propargyl bromide (80% in toluene) were purchased from Alfa Aesar and used without further purification. Merrifield Resin was purchased from GL Biochem (Shanghai) Ltd. and used as received. Triethylamine (TEA) and toluene were distilled over CaH_2. *p*-Hydroxybenzaldehyde, chlorobenzene, 3-chloro-1-propanol, dichloromethane, 2-propanol, and all other chemicals were purchased from Sinopharm Chemical Reagent Co. Ltd. and used as received. Tris(2-(dimethylamino)ethyl)amine (Me_6TREN),[53] 3-azido-1-propanol,[54] azido-functionalized Merrifield resin,[55] and 1-(2-propynyloxy)benzene[56] were prepared according to literature procedures.

Synthetic schemes employed for the synthesis of *alkynyl-C_{60}*, *C_{60}*-PNIPAM, (*C_{60}*)$_2$-PNIPAM, and PEG(-*C_{60}*)-*b*-PNIPAM are shown in Schemes 1, 2, and 3, respectively.

Synthesis of 2-(4-Ethynyloxyphenyl)-3,4-fulleropyrrolidine (Alkynyl-C_{60})[57]. *Alkynyl-C_{60}* was prepared by the reaction of C_{60} with 4-prop-2-ynyloxybenzaldehyde according to literature procedures.[57] To a stirred suspension of *p*-hydroxybenzaldehyde (1.832 g, 15 mmol) and K_2CO_3 (3.11 g, 22.5 mmol) in 80 mL of acetone, propargyl bromide (80 wt % in toluene) (2.34 g, 16 mmol) was added dropwise. The reaction mixture was stirred at reflux under nitrogen for 8 h. After cooling to room temperature, 150 mL of water was added, followed by extraction with CH_2Cl_2 (100 mL × 3). The combined organic layers were dried over anhydrous Na_2SO_4 and filtered. After removing all the solvents, the residues were further purified on a silica gel column using petroleum ether/ethyl acetate (3/1 v/v) as eluent, affording 4-prop-2-ynyloxybenzaldehyde. The product was obtained as white solid (2.21 g, yield: 93%). ^{1}H NMR ($CDCl_3$, δ, ppm, TMS): 9.91 (1H, C*H*O−Ph), 7.88 (2H, Ph−*H*), 7.11 (2H, Ph−*H*), 4.78 (2H, −OC*H*$_2$C≡CH), and 2.57 (1H, −OCHH$_2$C≡C*H*) (Figure S1). Next, 4-prop-2-ynyloxybenzaldehyde (0.474 g, 3.0 mmol), glycine (90 mg, 1.2 mmol), and C_{60} (0.432 g, 0.6 mmol) were dissolved in 150 mL of chlorobenzene; the reaction mixture was refluxed for 8 h under magnetic stirring. After cooling to room temperature, the solvents were removed using a rotary evaporator. The residues were further purified by silica gel column chromatography using toluene as the eluent, affording *alkynyl-C_{60}* (0.246 g, yield: 46%) as a black powder. ^{1}H NMR ($CDCl_3$, δ, ppm, TMS): 7.74 (2H, Ph−*H*), 7.05 (2H, Ph−*H*), 5.77 (1H, C_{60}−C*H*(NH)−Ph), 5.08 (1H, C_{60}−C*H*$_2$−NH−), 4.87 (1H, C_{60}−C*H*$_2$−NH−), 4.70 (2H, −OCH*H*$_2$C≡CH), 2.50 (1H, −OCHH$_2$C≡C*H*), and 1.57 (1H, C_{60}−CH$_2$−N*H*−) (Figure S1). Anal. Calcd for $C_{71}H_{11}NO$: C, 95.40; H, 1.24; N, 1.57. Found: C, 94.98; H, 1.15; N, 1.52.

Synthesis of 3-Azidopropyl 2-Bromoisobutyrate (APBIB)[54]. The ATRP initiator, APBIB, was prepared by the esterification reaction of 3-azido-1-propanol with 2-bromoisobutyryl bromide in the presence of TEA. A 250 mL round-bottom flask was charged with 3-azido-1-propanol (10.11 g, 0.10 mol), TEA (11.13 g, 0.11 mol), and dry CH_2Cl_2 (120 mL). The reaction mixture was cooled to 0 °C in an ice−water bath; 2-bromoisobutyryl bromide (25.29 g, 0.11 mol) in 30 mL of dry CH_2Cl_2 was added dropwise over a period of 1 h under magnetic stirring. After the addition was completed, the reaction mixture was stirred at 0 °C for 1 h and then at room temperature overnight. After filtration and removing all the solvents, the residues were further purified by a silica gel column chromatograph using CH_2Cl_2/petroleum ether (2:1 v/v) as eluent, affording APBIB as a colorless liquid (23.0 g, yield: 92%). ^{1}H NMR ($CDCl_3$, δ, ppm, TMS): 4.27 (2H, −COOC*H*$_2$CH$_2$CH$_2$N$_3$), 3.45 (2H, −COOCH$_2$CH$_2$C*H*$_2$N$_3$), 1.99 (2H, −COOCH$_2$C*H*$_2$CH$_2$N$_3$), and 1.94 (6H, −C(C*H*$_3$)$_2$−Br) (Figure S2).

*Synthesis of N_3-PNIPAM (**a1**)*. Typical procedures employed for the preparation of monoazide-terminated PNIPAM (**a1**) were described below. APBIB (80 mg, 0.32 mmol), NIPAM (5.43 g, 48 mmol), Me_6TREN (74 mg, 0.32 mmol), and 2-propanol (6 mL) were added into a reaction flask. The mixture was degassed by three freeze−pump−thaw cycles. After the solution temperature increased to 25 °C, CuCl (32 mg, 0.32 mmol) was introduced as a solid into the reaction flask to start the polymerization. The reaction solution became dark green and more viscous as polymerization proceeded. After 4.5 h, the conversion was about 66% as judged by ^{1}H NMR. The polymerization was quenched with $CuCl_2$, diluted with 20 mL of THF, and then exposed to air. The reaction mixture was passed through a silica gel column to remove the copper catalyst. After removing the solvents by a rotary evaporator, the residues were dissolved in THF and precipitated into an excess of ethyl ether. The above dissolution−precipitation cycle was repeated twice. The final product was dried in a vacuum oven at

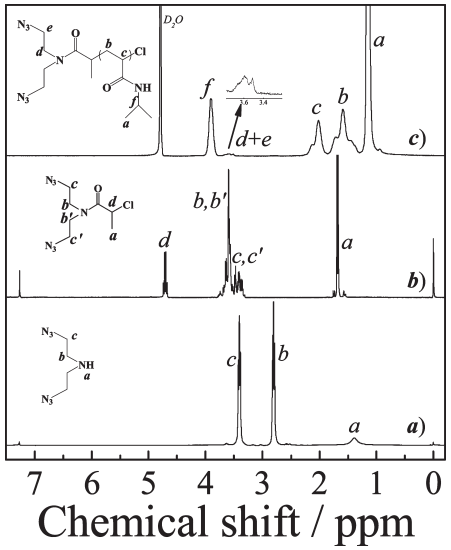

Figure 1. ^{1}H NMR spectra recorded for (a) $(N_3)_2$-*NH* in $CDCl_3$, (b) $(N_3)_2$-*Cl* in $CDCl_3$, and (c) $(N_3)_2$-PNIPAM$_{100}$ in D_2O.

room temperature, yielding a white solid (3.47 g, yield: 63%; $M_{n,GPC}$ = 10.1 kDa, M_w/M_n = 1.12). The actual DP of PNIPAM block was determined to be 98 by ^{1}H NMR analysis in D_2O (Figure S2). Thus, the product was denoted as N_3-PNIPAM$_{98}$.

Synthesis of $(N_3)_2$-*NH*[58]. To a stirred solution of sodium azide (14.6 g, 0.225 mol) in 150 mL of water was added bis(2-chloroethyl)amine hydrochloride (20.0 g, 0.112 mol). After stirring for 2 h at 90 °C, another potion of sodium azide (14.6 g) was added, and the reaction mixture was stirred for 48 h at 90 °C. After cooling to room temperature, the solution pH was adjusted to ca. 10 with aqueous NaOH (10 mol/L). The aqueous solution was extracted with ethyl ether (5 × 50 mL). The combined organic layers were dried over anhydrous Na_2SO_4, and the solvents were removed using a rotary evaporator. After distillation at reduced pressure, a colorless liquid was obtained (11.85 g, yield: 68.2%). (*Caution*: special care should be taken when heating the azide compound above 80−85 °C because it becomes shock-sensitive at elevated temperatures.) ^{1}H NMR ($CDCl_3$, δ, ppm, TMS): 3.42 (4H, N_3CH_2-), 2.79 (4H, $-CH_2NHCH_2-$), and 1.38 (1H, $-NH-$) (Figure 1).

Synthesis of N,N-*Bis(2-azidoethyl)-2-chloropropanamide (BACP)*. The ATRP initiator, BACP, was prepared by the amidation of $(N_3)_2$-*NH* with 2-chloropropionyl chloride in the presence of TEA. A 250 mL round-bottom flask was charged with $(N_3)_2$-*NH* (12.41 g, 0.08 mol), TEA (9.11 g, 0.09 mol), and dry CH_2Cl_2 (120 mL). The reaction mixture was cooled to 0 °C in an ice−water bath, and 2-chloropropionyl chloride (11.43 g, 0.09 mol) in 30 mL of CH_2Cl_2 was added dropwise over a period of 1 h under magnetic stirring. After the addition was completed, the reaction mixture was stirred at 0 °C for 1 h and then at room temperature for 15 h. After filtration and removing all the solvents, the residues were further purified by a silica gel column chromatograph using CH_2Cl_2/petroleum ether (3:1 v/v) as eluent, affording BACP as a colorless oil (18.47 g, yield: 94%). ^{1}H NMR ($CDCl_3$, δ, ppm, TMS): 4.75−4.65 (1H, $-CH(CH_3)-Cl$), 3.73−3.50 (4H, $-CON(CH_2CH_2N_3)_2$), 3.54−3.28 (4H, $-CON(CH_2CH_2N_3)_2$), and 1.73−1.62 ($-CH(CH_3)Cl$) (Figure 1).

Synthesis of $(N_3)_2$-*PNIPAM* (***b1***). A typical example for the preparation of **b1** is described below. BACP (79 mg, 0.32 mmol), NIPAM (5.43 g, 48 mmol), Me_6TREN (74 mg, 0.32 mmol), and 2-propanol (5 mL) were added into a reaction flask. The mixture was degassed by three freeze−pump−thaw cycles. After the temperature increased to 25 °C, CuCl (32 mg, 0.32 mmol) was introduced as a solid into the reaction flask to start the polymerization. The reaction solution became dark green and more viscous as polymerization proceeded. After 5 h, the conversion was about 67% as judged by ^{1}H NMR. The polymerization was quenched with $CuCl_2$, diluted with 20 mL of THF, and then exposed to air. The reaction mixture was passed through a silica gel column to remove the copper catalysts. After removing the solvents by a rotary evaporator, the residues were dissolved in THF and precipitated into an excess of ethyl ether. The above dissolution−precipitation cycle was repeated twice. The final product was dried in a vacuum oven at room temperature, yielding a white solid (3.58 g, yield: 65%; $M_{n,GPC}$ = 10.3 kDa, M_w/M_n = 1.12). The actual DP of PNIPAM block was determined to be 100 by ^{1}H NMR analysis in D_2O (Figure 1). Thus, the product was denoted as $(N_3)_2$-PNIPAM$_{100}$.

Synthesis of PEG-(N_3)-b-*PNIPAM* (***c1***). Detailed procedures employed for the preparation of monoalkynyl-terminated PEG, difunctional PEG terminated with a secondary amine moiety and azide group at the chain end, PEG-*NH*-N_3, and PEG-based difunctional initiator, PEG(-N_3)-*Cl*, are available in the Supporting Information (Scheme S1, Figures S8 and S9). Typical procedures employed for the synthesis of PEG-(N_3)-*b*-PNIPAM (**c1**) are described below. PEG(-N_3)-*Cl* difunctional macroinitiator (0.845 g, 0.16 mmol), NIPAM (1.45 g, 12.8 mmol), Me_6TREN (74 mg, 0.32 mmol), 2-propanol (4 mL), and DMF (1 mL) were added into a reaction flask. The solution mixture was degassed by two freeze−pump−thaw cycles. After the flask was thermostated at 40 °C, CuCl (32 mg, 0.32 mmol) was introduced as a solid into the reaction flask to start the polymerization. The solution turned dark green and apparently more viscous as polymerization proceeded. After 8 h, the monomer conversion was determined to be 88% as judged by ^{1}H NMR. The polymerization was quenched with $CuCl_2$, diluted with 20 mL of THF, and then exposed to air. The reaction mixture was passed through a silica gel column to remove the copper catalyst. After removing the solvents by a rotary evaporator, the residues were dissolved in THF and precipitated into an excess of ethyl ether. The above dissolution−precipitation cycle was repeated twice. The final product was dried in a vacuum oven at room temperature, yielding a white solid (2.05 g, yield: 89%). GPC analysis in THF gave an $M_{n,GPC}$ of 12.7 kDa and an M_w/M_n = 1.15. The actual DP of PNIPAM block was determined to be 70 by ^{1}H NMR analysis in D_2O. Thus, the polymer was denoted as PEG$_{113}$(-N_3)-*b*-PNIPAM$_{70}$.

Synthesis of C_{60}-*PNIPAM* (***a2***), $(C_{60})_2$-*PNIPAM* (***b2***), *and PEG(-*C_{60})-b-*PNIPAM* (***c2***). Target fullerenated diblock and homopolymers, **a2**, **b2**, and **c2**, were obtained by the click reaction of *alkynyl*-C_{60} with **a1**, **b1**, and **c1**, respectively (Schemes 2 and 3). Typical procedures employed for the synthesis of **b2** are as follows. The mixture of *alkynyl*-C_{60} (89 mg, 0.1 mmol), **b1** (0.116 g, 0.01 mmol), and toluene/DMF mixture (20 mL, 1:1 v/v) was subjected to one brief freeze−pump−thaw cycle; CuCl (5 mg, 0.05 mmol) was then introduced as a solid into the reaction flask. The reaction flask was carefully degassed by three freeze−pump−thaw cycles and placed in an oil bath thermostated at 50 °C. After stirring for 36 h, azide-functionalized Merrifield resin (0.188 g, 0.15 mmol azide moiety) was then added. The suspension was kept stirring for another 8 h at 50 °C. After suction filtration, the filtrate was diluted with THF and passed through a basic alumina column to remove the copper catalyst. After removing all the solvents at reduced pressure, the residues were dissolved in THF and precipitated into an excess of *n*-hexane. The above dissolution−precipitation cycle was repeated for three times to ensure the completely removal of unreacted *alkynyl*-C_{60}. The final product was dried in a vacuum oven overnight at room temperature, affording **b2** as a brown powder (115 mg, yield: 86%; $M_{n,GPC}$ = 10.7 kDa, M_w/M_n = 1.12). The preparation of **a2** and **c2** followed similar procedures as those described for **b2**, except that the amount of C_{60} and azide-functionalized Merrifield resin were halved. The molecular

Table 1. Molecular Parameters of Azido-Functionalized Precursors and Corresponding Fullerenated Polymers Synthesized in This Work

samples	DP_{theo} [a]	DP_{NMR} [b] PEG	DP_{NMR} [b] PNIPAM	M_n [c] (kDa)	PDI [c]	C_{60} (wt %) [d] calcd	C_{60} (wt %) [d] found
N_3-PNIPAM$_{98}$	99		98	10.1	1.12		
C_{60}-PNIPAM$_{98}$			98	10.5	1.12	5.9	5.6
$(N_3)_2$-PNIPAM$_{100}$	101		100	10.3	1.12		
$(C_{60})_2$-PNIPAM$_{100}$			100	10.7	1.12	10.8	10.3
PEG$_{113}$(-N_3)-*b*-PNIPAM$_{70}$	70	113	70	12.7	1.15		
PEG$_{113}$(-C_{60})-*b*-PNIPAM$_{70}$		113	70	12.7	1.15	5.1	4.8

[a] Calculated based on monomer conversion and [NIPAM]/[ATRP initiator] ratios. [b] Determined by ^{1}H NMR analysis in D_2O. [c] Obtained from GPC analysis using THF as eluent. [d] Determined by TGA analysis.

parameters of all azido-functionalized precursors and the corresponding fullerenated polymers prepared in this work are summarized in Table 1.

Characterization. *Nuclear Magnetic Resonance Spectroscopy (NMR)*. All NMR spectra were recorded on a Bruker AV300 NMR spectrometer (resonance frequency of 300 MHz for ^{1}H) operated in the Fourier transform mode. $CDCl_3$ and D_2O were used as the solvent.

Fourier Transform Infrared Spectroscopy (FT-IR). Fourier transform infrared (FT-IR) spectra were recorded on a Bruker VECTOR-22 IR spectrometer. The spectra were collected at 64 scans with a spectral resolution of 4 cm^{-1}.

Gel Permeation Chromatography (GPC). Molecular weights and molecular weight distributions were determined by gel permeation chromatography (GPC) equipped with a Waters 1515 pump, a Waters 2414 RI detector, and Waters UV/RI detectors (set at 30 °C). It used a series of three linear Styragel columns HR3, HR4, and HR6 at an oven temperature of 45 °C. The eluent was THF at a flow rate of 1.0 mL/min. A series of low-polydispersity polystyrene (PS) standards were employed for the GPC calibration.

Ultraviolet−Visible Spectroscopy (UV−vis). UV−vis absorption spectra and the temperature-dependent optical transmittance of the aqueous solution of C_{60}-PNIPAM$_{98}$, $(C_{60})_2$-PNIPAM$_{100}$, PEG$_{113}$(-C_{60})-*b*-PNIPAM$_{70}$, and their corresponding azide-containing precursors (2.0 g/L) at a wavelength of 700 nm were acquired on a Unico UV/vis 2802PCS spectrophotometer. A thermostatically controlled couvette was employed, and the heating rate was 0.2 °C min^{-1}.

Thermogravimetric Analysis (TGA). TGA was performed under a N_2 atmosphere at a heating rate of 10 °C /min from room temperature to 800 °C using a Perkin-Elmer Diamond TG/DTA.

Surface Tensiometry. Equilibrium surface tensions were measured using a JK99B tensiometer with a platinum plate. The measuring accuracy of the device as reported by the manufacturer is ±0.1 mN/m. The reported surface tension was the average of four to five measurements that were taken after allowing each of the solutions to equilibrate in the instrument at a temperature of 25.0 ± 0.2 °C.

Laser Light Scattering (LLS). A commercial spectrometer (ALV/DLS/SLS-5022F) equipped with a multi-tau digital time correlator (ALV5000) and a cylindrical 22 mW UNIPHASE He−Ne laser (λ_0 = 632 nm) as the light source was employed for dynamic and static laser light scattering (LLS) measurements. Scattered light was collected at a fixed angle of 90° for duration of ~10 min. Distribution averages and particle size distributions were computed using cumulants analysis and CONTIN routines. All data were averaged over three measurements.

Transmission Electron Microscopy (TEM). TEM observations were conducted on a Hitachi H-800 electron microscope at an acceleration voltage of 200 kV. The sample for TEM observations was prepared by placing 10 μL of micellar solution on copper grids coated with thin films of Formvar and carbon successively.

Results and Discussion

Synthesis of C_{60}-Embedded Water-Soluble Block Copolymer and Homopolymers. Synthetic schemes employed for the preparation of C_{60}-PNIPAM (**a2**), $(C_{60})_2$-PNIPAM (**b2**), and PEG(-C_{60})-*b*-PNIPAM (**c2**) are shown in Schemes 1−3 and Scheme S1, which takes advantage of the high efficiency, quantitative yield, and relatively mild reaction conditions of click chemistry.[59,60] The reaction of 4-prop-2-ynyloxy-benzaldehyde with pristine C_{60} in the presence of glycine afforded alkynyl-modified C_{60}, *alkynyl*-C_{60}. Next, azide-containing polymer precursors including monoazide-terminated and α,α-diazide-terminated PNIPAM, N_3-PNIPAM (**a1**) and $(N_3)_2$-PNIPAM (**b1**), as well as PEG-*b*-PNIPAM with one azide moiety at the diblock junction, PEG(-N_3)-*b*-PNIPAM (**c1**), were synthesized via ATRP using specific azide-functionalized small molecule and polymeric initiators. The subsequent click reaction of **a1**, **b1**, and **c1** with *alkynyl*-C_{60} led to the successful preparation of thermoresponsive diblock copolymer and homopolymers functionalized with controlled numbers of C_{60} at designated positions, including C_{60}-PNIPAM (**a2**), $(C_{60})_2$-PNIPAM (**b2**), and PEG(-C_{60})-*b*-PNIPAM (**c2**).

Monoazide- and diazide-based small molecule initiators, APBIB and BACP, were prepared by the esterification and amidation reaction of 3-azido-1-propanol and N,N-bis(2-azidoethyl)amine, $(N_3)_2$-*NH*, with an excess of 2-bromoisobutyryl bromide and 2-chloropropionyl chloride, respectively. $(N_3)_2$-*NH* was prepared by the azidation of bis(2-chloroethyl) amine hydrochloride. Figure 1b shows the ^{1}H NMR spectrum of BACP together with the peak assignments. The integral ratio of peak *a* (1.73−1.62 ppm, −CH(CH_3)Cl) to that of peaks *b* and *c* in the range of 3.73−3.28 ppm [*b*: −CON-(CH_2CH_2N$_3$)$_2$; *c*: −CON(CH$_2$CH_2N$_3$)$_2$] was calculated to be ca. 3:8. Moreover, in comparison with the ^{1}H NMR spectrum of $(N_3)_2$-*NH* (Figure 1a), the signals at δ = 2.92−2.66 ppm (−CH_2NH−) completely disappeared in the ^{1}H NMR spectrum of BACP. These results indicated the successful preparation of BACP. According to similar procedures, APBIB initiator was also successfully prepared (Figure S2).

APBIB and BACP were then employed as initiators for the ATRP of NIPAM in the presence of CuCl/Me$_6$TREN catalyst in 2-propanol at 25 °C. The controlled polymerization of NIPAM via the ATRP technique has been well-documented previously.[61−66] Typical THF GPC trace of **b1** is shown in Figure 2a, giving an $M_{n,GPC}$ of 10.3 kDa and an M_w/M_n of 1.12. The actual DP of **b1** was determined to be 100 by ^{1}H NMR (Figure 1c) by comparing integration areas of peaks *d* and *e* in the range of 3.73−3.28 ppm to that of peak *f* at δ = 3.9 ppm. Thus, the obtained α,α-diazide-terminated product was denoted as $(N_3)_2$-PNIPAM$_{100}$. Moreover, the presence of azide groups in **b1** is also clearly evident by the presence of characteristic azide absorbance peak at ~2100 cm^{-1} in its FT-IR spectrum (Figure 3a).

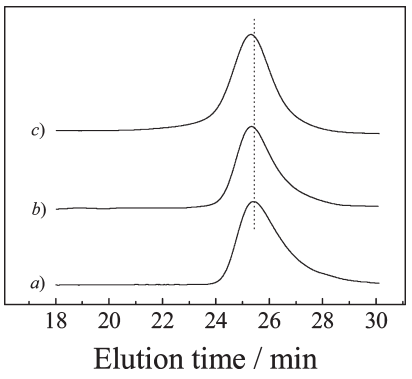

Figure 2. THF GPC traces of (a) $(N_3)_2$-PNIPAM$_{100}$ detected by RI detector, (b) $(C_{60})_2$-PNIPAM$_{100}$ detected by RI detector, and (c) $(C_{60})_2$-PNIPAM$_{100}$ detected by UV detector at 330 nm.

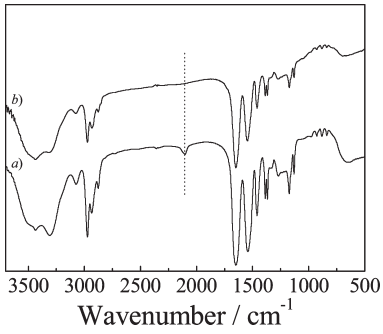

Figure 3. FT-IR spectra recorded for (a) $(N_3)_2$-PNIPAM$_{100}$ and (b) $(C_{60})_2$-PNIPAM$_{100}$.

In order to obtain monoazide-terminated PNIPAM (**a1**) with a DP close to that of **b1**, the monomer conversion of the ATRP of NIPAM using APBIB as initiator was controlled by adjusting the reaction time. Since in typical ATRP process APBIB serves as a faster initiating species than that of BACP due to the weaker C−Br bond in the former, CuCl was used as the catalyst via the halide exchange mechanism to further enhance the initiating efficiency.[67] The actual DP of **a1** was determined to be 98 by the integral ratio of peak e at δ = 3.9 ppm and peak *d* at δ = 3.45 ppm from its ^{1}H NMR spectrum (Figure S2b). Thus, the monoazide-terminated PNIPAM was denoted as N_3-PNIPAM$_{98}$. THF GPC analysis gave an M_n of 10.1 kDa and an M_w/M_n of 1.12 for **a1**. The FT-IR spectrum of **a1** (Figure S3) also revealed the presence of characteristic azide absorption peak at ~2100 cm^{-1}.

Recently, Perrier et al.[68] reported that azide moieties could react with double bonds of NIPAM in the absence of copper catalysts at high temperature (60 °C) for extended time periods (20 h). They also noted that side reactions can be eliminated by reducing polymerization temperatures and shortening the reaction time. Benicewicz et al.[69] and Bai et al.[70] also demonstrated that azide moieties just react with double bond of monomers at elevated temperatures and no reaction can occur at room temperature. It should be noted that in the current work ATRP syntheses of N_3-PNIPAM and $(N_3)_2$-PNIPAM were conducted at 25 °C for duration of 4.5 and 5 h, respectively. However, the phenomenon reported by Perrier et al. indeed poses uncertainties, i.e., the possible loss of azide terminal functionalities during the ATRP process.

Further work has been conducted to determine end-group functionality of $(N_3)_2$-PNIPAM (Scheme S2), which was chosen as a representative example as it possess two azide moieties at the chain terminal. Detailed experimental procedures and results are included in the Supporting Information. The click reaction of $(N_3)_2$-PNIPAM with an excess of 1-(2-propynyloxy)benzene afforded $(Ph)_2$-PNIPAM. Typical ^{1}H NMR spectra recorded for $(N_3)_2$-PNIPAM and $(Ph)_2$-PNIPAM are shown in Figure S8. A comparison of the ^{1}H NMR spectra of $(N_3)_2$-PNIPAM and $(Ph)_2$-PNIPAM revealed that after click reaction peaks *b* and *c* (3.7−3.4 ppm; 8H, $N_3CH_2CH_2-$) in the former completely disappeared, whereas a new resonance signal at 4.7 ppm (peak *c*; 4H, triazole$-CH_2CH_2$) in the NMR spectrum of $(Ph)_2$-PNIPAM can be clearly discerned. Moreover, the integral ratio between peak *e* (5.2 ppm; 4H, PhOCH_2-triazole) to that of peak *c* was determined to be close to unity (Figure S8, *b*). Considering the contribution of trizaole-CH_2CH_2N- in the region of ~4.0 ppm, the DP of $(Ph)_2$-PNIPAM can be calculated to be 100, which exactly agrees with that determined before click labeling with 1-(2-propynyloxy)benzene. On the basis of the above results, we can conclude that the loss of azide functionality during the ATRP of NIPAM under current conditions (~5 h, 25 °C) is negligible.

PEG(-N_3)-*b*-PNIPAM (**c1**) was obtained via a multistep synthesis, starting from PEG$_{113}$-OH and bis(2-azidoethyl) amine, $(N_3)_2$-*NH* (Scheme S1). Click reaction of monoalkynyl-terminated PEG with an excess of trifunctional core molecule $(N_3)_2$-*NH* afforded difunctional PEG possessing an azido and a secondary amine moiety at the chain end, PEG-*NH*-N_3.[58] The molar ratio of $(N_3)_2$-*NH* to that of monoalkynyl-terminated PEG was fixed at 50:1, and the click conditions (polymer concentration and reaction temperature) were optimized to eliminate the possible coupling reaction of PEG chains by $(N_3)_2$-*NH*. Relevant experimental details are included in the Supporting Information (Figures S9 and S10). The subsequent ATRP of NIPAM using PEG(-N_3)-*Cl* as the macroinitiator led to PEG(-N_3)-*b*-PNIPAM bearing an azido moiety at the diblock junction point. THF GPC analysis gave an $M_{n,GPC}$ of 12.7 kDa and an M_w/M_n = 1.15. The actual DP of PNIPAM block was determined to be 70 by ^{1}H NMR analysis in D_2O. Thus, the product was denoted as PEG$_{113}$(-N_3)-*b*-PNIPAM$_{70}$.

Finally, the click reaction of *alkynyl*-C_{60} with **a1**, **b1**, and **c1** led to the facile preparation of well-defined fullerenated water-soluble polymers, **a2**, **b2**, and **c2**. To ensure complete consumption of azide moieties in azide-containing precursors, excess *alkynyl*-C_{60} (5 times molar excess relative to azide moieties) was used in all three cases. In Cheng's work,[40] excess alkynyl-functionalized fullerene was also used to ensure the complete reaction of azide moieties of PS-N_3, and the product was purified by column chromatograph. To simplify the procedure of removing excess *alkynyl*-C_{60}, we choose to purify the product by "clicking" onto azide-functionalized Merrifield resin, followed by a simple filtration step.[55] Thus, in our case click chemistry also provides a facile purification method to remove excess C_{60} precursor. It should be noted that in typical thermal [3 + 2] cycloaddition reaction of pristine C_{60} with azide-containing species tedious procedures were typically needed to remove excess C_{60}. Moreover, the click reactions of *alkynyl*-C_{60} with **a1**, **b1**, and **c1** were conducted at 50 °C, which is much lower than that employed in typical thermal [3 + 2] cycloaddition reaction between azido-functionalized polymers and pristine C_{60} (~130 °C). Under the current conditions, we can safely ensure that multiadduction of azide-functionalized precursor chains onto *alkynyl*-C_{60} will not occur. Most importantly, the click reaction *alkynyl*-C_{60} with $(N_3)_2$-PNIPAM will yield PNIPAM(-N_3)-C_{60} at first. The relatively low temperature employed for the click reaction can also avoid

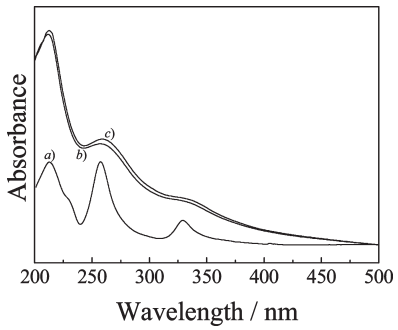

Figure 4. UV−vis absorption spectra recorded for (a) pristine C_{60} in *n*-hexane, (b) C_{60}-PNIPAM$_{98}$ and (c) $(C_{60})_2$-PNIPAM$_{100}$ in aqueous solution.

the intramolecular thermal [3 + 2] cycloaddition reaction, which is highly possible at elevated temperatures due to the close neighboring of azide moiety and C_{60} in PNIPAM-(-N_3)-C_{60}.

After click reactions, the complete disappearance of characteristic azide absorption peak at ~2100 cm^{-1} in the FT-IR spectra of **a2**, **b2**, and **c2** (Figure 3 and Figure S3), as compared to those of **a1**, **b1**, and **c1**, clearly confirmed the complete consumption of azide moieties. Moreover, the obtained brown powders of **a2**, **b2**, and **c2** are soluble in common organic solvents such as toluene, THF, chloroform, DMF, methanol, and dichloromethane as well as in water. The dramatically improved solubility partially confirmed the successful conjugation of *alkynyl*-C_{60} onto azide-containing polymer precursors. It should be noted that the click reactions were conducted in a toluene/DMF mixture (1:1 v/v) under ligand-free conditions. It has been established previously that the click reaction can be quite efficient even in the absence of ligand if the solvent can facilitate sufficient solubility of copper catalyst.[71]

Typical GPC traces of **b2** detected by RI and UV dual detectors are shown in Figure 2. Both GPC traces of **b2** showed monomodal elution peaks by using RI and UV detectors, yielding an $M_{n,GPC}$ of 10.7 kDa and an M_w/M_n = 1.12. Compared to that of the α,α-diazide-terminated precursor (**b1**), the slight shift to higher MW side in the elution peak of **b2** suggested the presence of C_{60} species. In previous literature reports, the end-functionalization of polymer chain with C_{60} also yielded a discernible GPC shift compared to the precursor.[14−18,28,32] The absence of shoulder peak in the high-MW side supported the conclusion that there was no discernible multiple addition product. It should be noted that the α,α-diazide-terminated precursor (**b1**) exhibit no absorbance at ~330 nm. The similar shape and comparable elution times between GPC elution peaks detected by UV (330 nm wavelength, characteristic absorbance peak of C_{60}) and RI detectors for **b2** further confirmed the presence of C_{60} and a high degree of end-group functionality, as only the C_{60} moiety in **b2** can be detected by both UV (λ = 330 nm) and RI detectors.[14−18,32]

The weight percentages of C_{60} in **a2**, **b2**, and **c2** were then determined to be 5.6, 10.3, and 4.8 wt % by TGA analysis, respectively (Table 1). These were in reasonable agreement with those calculated from chemical structures of **a2**, **b2**, and **c2** (Schemes 2 and 3), which suggested that predetermined numbers of C_{60} moiety were incorporated into PNIPAM-based diblock copolymer and homopolymers.[14−18,32] The presence of C_{60} in **a2**, **b2**, and **c2** has been further confirmed by UV−vis spectroscopy (Figure 4 and Figure S5). C_{60} exhibits characteristic absorption peaks at 214, 256, and 330 nm in *n*-hexane.[14−18,28,32] From Figure 4, it is clearly evident that both **a2** and **b2** in aqueous solution have three characteristic absorption peaks at 212, 258, and 333 nm. Compared to their azide-containing precursors (**a1** and **b1**), these peaks can be ambiguously ascribed to the presence of C_{60}. Similar conclusion can also be obtained for **c2**, as evidenced from Figure S5.

On the basis of the above results, we can conclude that well-defined water-soluble fullerenated PNIPAM-based diblock and homopolymers functionalized with controllable numbers of C_{60} at predetermined positions were successfully prepared via a combination of ATRP and click reactions. In the subsequent section, we further investigated their supramolecular self-assembling behavior in aqueous solution and the corresponding thermo-induced collapse/aggregation of C_{60}-incorporated hybrid nanoparticles due to the thermoresponsiveness of PNIPAM chains.

Self-Assembly of C_{60}-Functionalized Water-Soluble Block Copolymer and Homopolymers in Aqueous Solution. C_{60}-PNIPAM$_{98}$ (**a2**), $(C_{60})_2$-PNIPAM$_{100}$ (**b2**), and PEG$_{113}$(-C_{60})-*b*-PNIPAM$_{70}$ (**c2**) contain highly hydrophobic C_{60} species and thermoresponsive water-soluble PNIPAM segments. In particular, to the best of our knowledge, PEG$_{113}$(-C_{60})-*b*-PNIPAM$_{70}$ represents the first example of double hydrophilic block copolymer (DHBC) embedded with a C_{60} moiety at the diblock junction.[11,72,73] Previously, we reported the synthesis and self-assembly of an amphiphilic diblock copolymer incorporated with C_{60} at the diblock junction point, PEG(-C_{60})-*b*-PS.[28] Upon properly tuning the relative block lengths between PEG and PS, the hybrid block copolymer can self-assemble into well-defined vesicular aggregates in aqueous solution. In the self-assembled vesicles, C_{60} moieties were located at the both the inner and outer sides of vesicle bilayers. Very recently, Liu et al. also reported the synthesis of hybrid amphiphilic block copolymers bearing a C_{60} moiety at the diblock junction via ATRP technique.[39]

In aqueous solution, it is well-known that C_{60} moieties can undergo self-association due to hydrophobic interactions and strong $\pi-\pi$ stacking effects between C_{60} molecules.[14−18,29,37] On the other hand, PNIPAM homopolymer undergoes a coil-to-globule phase transition in dilute aqueous solution above its lower critical solution temperature (LCST).[45−52] On the basis of chemical intuition, C_{60}-PNIPAM$_{98}$ (**a2**), $(C_{60})_2$-PNIPAM$_{100}$ (**b2**), and PEG$_{113}$(-C_{60})-*b*- PNIPAM$_{70}$ (**c2**) should self-assemble into core−shell micellar structures consisting of hydrophobic cores of C_{60} molecules and hydrophilic PNIPAM coronas (**a2** and **b2**) or hydrophilic PEG/PNIPAM mixed coronas (**c2**) in aqueous solution at room temperature. At elevated temperatures above the LCST of PNIPAM, the originally formed aggregates at lower temperatures should undergo further structural arrangements due to the collapse/aggregation of PNIPAM segments. We further employed LLS, TEM, and temperature-dependent optical transmittance to characterize the self-assembled aggregates of **a2**, **b2**, and **b2** in aqueous solution.

*Self-Assembly of **a2** and **b2** in Aqueous Solution.* As C_{60}-PNIPAM$_{98}$ (**a2**) and $(C_{60})_2$-PNIPAM$_{100}$ (**b2**) possess comparable DP for PNIPAM segments, these two samples can serve as an excellent system to investigate the effects of C_{60} contents at terminal position of PNIPAM chains on their self-assembling behavior. Both hybrid polymers can be directly soluble in water. Critical aggregation concentrations (cac) of **a2** and **b2** in aqueous solution were determined to be 9.6×10^{-3} and 5.7×10^{-3} g/L by surface tensiometry measurements, respectively (Figure 5). Compared to **a2**, the lower cac of **b2** should be ascribed to the presence of two C_{60} moieties at the chain terminal, which drives

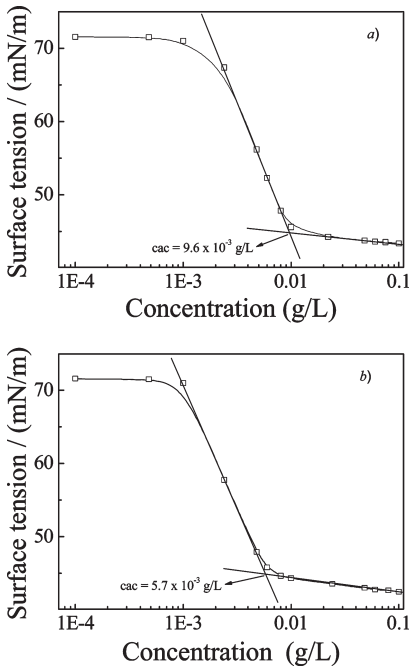

Figure 5. Determination of critical aggregation concentration (cac) from the experimental surface tension (γ) vs logarithm concentrations of (a) C_{60}-PNIPAM$_{98}$ and (b) $(C_{60})_2$-PNIPAM$_{100}$ in water at 25 °C.

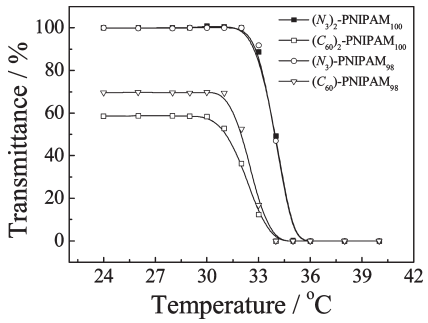

Figure 6. Temperature dependence of optical transmittance at 700 nm obtained for 2.0 g/L aqueous solutions of N_3-PNIPAM$_{98}$, C_{60}-PNIPAM$_{98}$, $(N_3)_2$-PNIPAM$_{100}$, and $(C_{60})_2$-PNIPAM$_{100}$.

the hydrophilic−hydrophobic balance to the hydrophobic side.

The temperature-dependent optical transmittance at 700 nm obtained for 2.0 g/L aqueous solution of **a2** and **b2** is shown in Figure 6. For comparison, relevant data of **a1** and **b1** were also incorporated. Aqueous solutions of **a1** and **b1** are transparent at room temperature, and the optical transmittance dramatically decreases above ~32 °C due to the LCST phase behavior. On the other hand, aqueous solutions of **a2** and **b2** exhibit opitical transmittances of ~50−70% at room temperature and a wavelength of 700 nm. Since C_{60} moieties possess no absorption at 700 nm, the relatively low optical transmittance might be ascribed to the presence of self-assembled aggregates due to the hydrophobicity of C_{60}. Upon heating to above ~30 °C, aqueous solutions of **a2** and **b2** exhibit considerable decrease in transmittance. The lower aggregation temperature of **a2** and **b2** in aqueous solutions compared to those of **a1** and **b1** can again be ascribed to the presence of hydrophobic C_{60} moieties. Geckeler et al.[37] and Yajima et al.[29] also found that C_{60}-PNIPAM retains the thermoresponsiveness of the PNIPAM precusor. The effects of end-group hydrophobicity on the phase transition of PNIPAM have been extensively investigated by Stover and co-workers.[61]

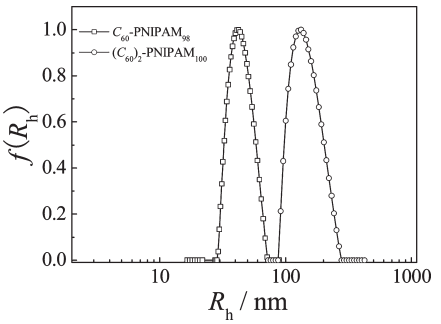

Figure 7. Hydrodynamic radius distributions, $f(R_h)$, obtained for 0.5 g/L aqueous solutions of C_{60}-PNIPAM$_{98}$ and $(C_{60})_2$-PNIPAM$_{100}$ at 25 °C.

Dynamic and static LLS were then used to characterize aggregates formed from **a2** and **b2** in aqueous solutions at 25 °C and a polymer concentration of 0.5 g/L. Figure 7 shows typical plots of the hydrodynamic radius distribution, $f(R_h)$, for C_{60}-containing hybrid nanoparticles self-assembled from **a2** and **b2**. R_h of the hybrid nanoparticles of **a2** is in the range of 29−71 nm, with an average hydrodynamic radius, $\langle R_h \rangle$, of 42 nm and a polydispersity index of size distribution, μ_2/Γ^2, of 0.13. On the other hand, **b2** self-assembles into hybrid nanoparticles with R_h in the range of 91−246 nm, yielding a $\langle R_h \rangle$ of 118 nm and μ_2/Γ^2 of 0.18. The apparent molar mass ($M_{w,app}$) determined by static LLS for **b2** (6.93×10^6 g/mol) is ca. 4 times larger than that for **a2** ($M_{w,app} \sim 1.57 \times 10^6$ g/mol). The average aggregation numbers, N_{agg}, of the aggregates formed by **a2** and **b2** were then calculated to be ~110 and ~460, respectively. The presence of two C_{60} moieties in **b2** should contribute to its larger $\langle R_h \rangle$ and N_{agg}, as compared to those of **a2**.

TEM observations were performed to examine the actual morphologies of the C_{60}-containing hybrid nanoparticles prepared by drying the aqueous solutions of **a2** and **b2** at 25 °C (Figure 8). Both images clearly revealed the presence of spherical nanoparticles with diameters in the range of 30−50 and 50−120 nm for samples prepared from **a2** and **b2**, respectively. The results were in reasonable agreement with those determined by dynamic LLS (Figure 7). TEM determines the micelle dimensions in the dry state, while dynamic LLS reports the intensity-average dimensions of nanoparticles in solution which contains considerable contribution from hydrophilic segment coronas.

*Self-Assembly of PEG$_{113}$(-C_{60})-b-PNIPAM$_{70}$ (**c2**) in Aqueous Solution.* PEG$_{113}$(-C_{60})-*b*-PNIPAM$_{70}$ represents the first example of DHBC embedded with a C_{60} moiety at the diblock junction. DHBCs can be directly dispersed in aqueous solution at certain conditions; upon changing the external conditions, such as pH, temperature, and ionic strength, one of the blocks of DHBCs can be selectively rendered water-insoluble, while the other block still remains well-solvated to stabilize the formed colloidal aggregates.[74−92] It is noteworthy that the self-assembly of PEG-*b*-PNIPAM diblock copolymer has been extensively investigated recently.[93−97] Because of the presence of thermoresponsive PNIPAM and hydrophilic PEG segments in **c2**, two micellar states might exist in aqueous solution depending on the temperatures due to the LCST phase transition of PNIPAM blocks. Dynamic and static LLS were then used to characterize the self-assembled aggregates of PEG$_{113}$(-C_{60})-*b*-PNIPAM$_{70}$ in aqueous solution.

At 25 °C and a polymer concentration of 0.2 g/L, micelles consisting of hydrophobic cores of C_{60} stabilized with mixed PEG/PNIPAM coronas with a $\langle R_h \rangle$ of 54 nm formed. Upon

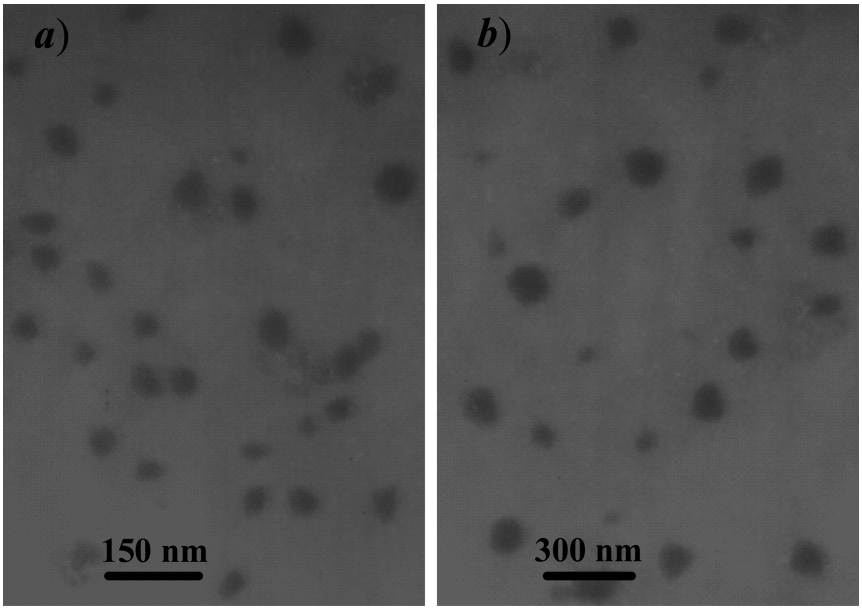

Figure 8. Typical TEM images obtained by drying 0.5 g/L aqueous solutions of (a) C_{60}-PNIPAM$_{98}$ and (b) $(C_{60})_2$-PNIPAM$_{100}$.

heating to 50 °C, another type of aggregate consisting of mixed C_{60}/PNIPAM cores and well-solvated PEG coronas with a $\langle R_h \rangle$ of 19 nm formed (Figure S6). The decrease of aggregate sizes at elevated temperatures should be ascribed to the collapse and aggregation of PNIPAM segments. Figure S7 shows the temperature dependence of $\langle R_h \rangle$ and $M_{w,app}$ of C_{60}-containing hybrid nanoparticle prepared from **c2**. $\langle R_h \rangle$ remains almost constant at ca. 54 nm below 35 °C; above that, aggregate sizes start to decrease and $\langle R_h \rangle$ stabilizes at ~20 nm above 45 °C. This clearly indicates the structural arrangement of the initially formed loose aggregates consisting of C_{60} cores at lower temperatures. Above the phase transition of PNIPAM blocks, the collapse and aggregation of PNIPAM can drive the spontaneous self-organization.

To further verify this, temperature-dependent $M_{w,app}$ of hybrid nanoparticles of **c2** was also plotted in Figure S7. $M_{w,app}$ remains almost constant at about 9.0×10^5 in the lower temperature range of 25−35 °C. At elevated temperatures, $M_{w,app}$ exhibits a considerable increase and stabilizes above ~50 °C. The average aggregation number, N_{agg}, of hybrid nanoparticles self-assembled from **c2** in aqueous solution was calculated to be 60 and 180 at 25 and 50 °C, respectively. The larger $\langle R_h \rangle$ and lower N_{agg} for aggregates formed at lower temperature reflect that they possess a quite loose structure. Above the LCST, both the hydrophobicity of C_{60} and PNIPAM contributed to the formation of well-defined and relatively compact aggregates.

Conclusion

We prepared thermoresponsive water-soluble diblock copolymer and homopolymers functionalized with controlled numbers of C_{60} moieties at designated positions via the combination of atom transfer radical polymerization and click chemistry. Alkynyl-functionalized C_{60} (*alkynyl*-C_{60}) and azide-containing polymer precursors including monoazide-terminated and α, α-diazide-terminated PNIPAM, N_3-PNIPAM and $(N_3)_2$-PNIPAM as well as PEG(-N_3)-*b*-PNIPAM bearing one azide moiety at the diblock junction were synthesized at first. The target hybrid thermoresponsive diblock copolymer and homopolymers, C_{60}-PNIPAM, $(C_{60})_2$-PNIPAM, and PEG(-C_{60})-*b*-PNIPAM, were then obtained via the click reaction of *alkynyl*-C_{60} with azide-containing precursors, including C_{60}-PNIPAM, $(C_{60})_2$-PNIPAM and PEG(-C_{60})-*b*-PNIPAM. C_{60}-containing spherical hybrid nanoparticles were fabricated via supramolecular self-assembly of C_{60}-PNIPAM, $(C_{60})_2$-PNIPAM, and PEG(-C_{60})-*b*-PNIPAM in aqueous solution. All these novel fullerenated polymers retain the thermoresponsiveness of PNIPAM-based precursors, and self-assembled hybrid nanoparticles exhibit thermo-induced collapse/aggregation behavior due to the LCST phase transition of PNIPAM segments.

Acknowledgment. The financial support of National Natural Scientific Foundation of China (NNSFC) Projects (20534020, 20674079, and 20874092), Specialized Research Fund for the Doctoral Program of Higher Education (SRFDP), and the Program for Changjiang Scholars and Innovative Research Team in University (PCSIRT) is gratefully acknowledged.

Supporting Information Available: Experimental details of the preparation of monoalkynyl-terminated PEG, PEG-*NH*-N_3, PEG(-N_3)-*Cl*, and $(Ph)_2$-PNIPAM; additional ^{1}H NMR, FT-IR, GPC, UV−vis, and LLS characterization results. This material is available free of charge via the Internet at http://pubs.acs.org.

References and Notes

(1) Kroto, H. W.; Allaf, A. W.; Balm, S. P. *Chem. Rev.* **1991**, *91*, 1213–1235.
(2) Wudl, F. *Acc. Chem. Res.* **1992**, *25*, 157–161.
(3) Ruoff, R. S.; Malhotra, R.; Huestis, D. L.; Tse, D. S.; Lorents, D. C. *Nature (London)* **1993**, *362*, 140–141.
(4) Bianco, A.; Da Ros, T.; Prato, M.; Toniolo, C. *J. Pept. Sci.* **2001**, *7*, 208–219.
(5) Da Ros, T.; Prato, M. *Chem. Commun.* **1999**, 663–669.
(6) Diederich, F.; Thilgen, C. *Science* **1996**, *271*, 317–323.
(7) Murthy, C. N.; Geckeler, K. E. *Chem. Commun.* **2001**, 1194–1195.
(8) Nakamura, E.; Isobe, H. *Acc. Chem. Res.* **2003**, *36*, 807–815.
(9) Samal, S.; Geckeler, K. E. *Chem. Commun.* **2000**, 1101–1102.
(10) Samal, S.; Choi, B. J.; Geckeler, K. E. *Chem. Commun.* **2000**, 1373–1374.
(11) Vitalini, D.; Spina, E.; Dattilo, S.; Mineo, P.; Scamporrino, E. *J. Polym. Sci., Part A: Polym. Chem.* **2008**, *46*, 2145–2153.
(12) Geckeler, K. E.; Hirsch, A. *J. Am. Chem. Soc.* **1993**, *115*, 3850–3851.
(13) Sun, Y. P.; Lawson, G. E.; Huang, W. J.; Wright, A. D.; Moton, D. K. *Macromolecules* **1999**, *32*, 8747–8752.

(14) Dai, S.; Ravi, P.; Tan, C. H.; Tam, K. C. *Langmuir* **2004**, *20*, 8569–8575.
(15) Teoh, S. K.; Ravi, P.; Dai, S.; Tam, K. C. *J. Phys. Chem. B* **2005**, *109*, 4431–4438.
(16) Ravi, P.; Wang, C.; Dai, S.; Tam, K. C. *Langmuir* **2006**, *22*, 7167–7174.
(17) Wang, C.; Ravi, P.; Tam, K. C. *Langmuir* **2006**, *22*, 2927–2930.
(18) Ravi, P.; Dai, S.; Tan, C. H.; Tam, K. C. *Macromolecules* **2005**, *38*, 933–939.
(19) Giacalone, F.; Martin, N. *Chem. Rev.* **2006**, *106*, 5136–5190.
(20) Wang, C. C.; Guo, Z. X.; Fu, S. K.; Wu, W.; Zhu, D. B. *Prog. Polym. Sci.* **2004**, *29*, 1079–1141.
(21) Hawker, C. J. *Macromolecules* **1994**, *27*, 4836–4837.
(22) Huang, X. D.; Goh, S. H.; Lee, S. Y. *Macromol. Chem. Phys.* **2000**, *201*, 2660–2665.
(23) Goh, H. W.; Goh, S. H.; Xu, G. Q. *J. Polym. Sci., Part A: Polym. Chem.* **2002**, *40*, 1157–1166.
(24) Huang, X. D.; Goh, S. H. *Macromolecules* **2000**, *33*, 8894–8897.
(25) Barrau, S.; Heiser, T.; Richard, F.; Brochon, C.; Ngov, C.; van de Wetering, K.; Hadziioannou, G.; Anokhin, D. V.; Ivanov, D. A. *Macromolecules* **2008**, *41*, 2701–2710.
(26) Li, L.; Wang, C. C.; Long, Z. H.; Fu, S. K. *J. Polym. Sci., Part A: Polym. Chem.* **2000**, *38*, 4519–4523.
(27) Stoilova, O.; Jerome, C.; Detrembleur, C.; Mouithys-Mickalad, A.; Manolova, N.; Rashkov, I.; Jerome, R. *Chem. Mater.* **2006**, *18*, 4917–4923.
(28) Wang, X. F.; Zhang, Y. F.; Zhu, Z. Y.; Liu, S. Y. *Macromol. Rapid Commun.* **2008**, *29*, 340–346.
(29) Tamura, A.; Uchida, K.; Yajima, H. *Chem. Lett.* **2006**, *35*, 282–283.
(30) Ford, W. T.; Nishioka, T.; McCleskey, S. C.; Mourey, T. H.; Kahol, P. *Macromolecules* **2000**, *33*, 2413–2423.
(31) Weis, C.; Friedrich, C.; Mulhaupt, R.; Frey, H. *Macromolecules* **1995**, *28*, 403–405.
(32) Zhou, P.; Chen, G. Q.; Hong, H.; Du, F. S.; Li, Z. C.; Li, F. M. *Macromolecules* **2000**, *33*, 1948–1954.
(33) Shen, X. F.; He, X. R.; Chen, G. Q.; Zhou, P.; Huang, L. *Macromol. Rapid Commun.* **2000**, *21*, 1162–1165.
(34) Ederle, Y.; Mathis, C. *Macromolecules* **1997**, *30*, 2546–2555.
(35) Kawauchi, T.; Kumaki, J.; Yashima, E. *J. Am. Chem. Soc.* **2005**, *127*, 9950–9951.
(36) Kawauchi, T.; Kumaki, J.; Yashima, E. *J. Am. Chem. Soc.* **2006**, *128*, 10560–10567.
(37) Zhou, G.; Harruna, I. I.; Zhou, W. L.; Aicher, W. K.; Geckeler, K. E. *Chem.—Eur. J.* **2007**, *13*, 569–573.
(38) Iwamoto, Y.; Yamakoshi, Y. *Chem. Commun.* **2006**, 4805–4807.
(39) Liu, Y.-L.; Chang, Y.-H.; Chen, W.-H. *Macromolecules* **2008**, *41*, 7857–7862.
(40) Zhang, W. B.; Tu, Y.; Ranjan, R.; Van Horn, R. M.; Leng, S.; Wang, J.; Polce, M. J.; Wesdemiotis, C.; Quirk, R. P.; Newkome, G. R.; Cheng, S. Z. D. *Macromolecules* **2008**, *41*, 515–517.
(41) Kolb, H. C.; Finn, M. G.; Sharpless, K. B. *Angew. Chem., Int. Ed.* **2001**, *40*, 2004–2021.
(42) Binder, W. H.; Sachsenhofer, R. *Macromol. Rapid Commun.* **2007**, *28*, 15–54.
(43) Fournier, D.; Hoogenboom, R.; Schubert, U. S. *Chem. Soc. Rev.* **2007**, *36*, 1369–1380.
(44) Lutz, J. F. *Angew. Chem., Int. Ed.* **2007**, *46*, 1018–1025.
(45) Heskin, M.; Guillet, J. E. *J. Macromol. Sci., Chem.* **1968**, *A2*, 1441–1455.
(46) Kubota, K.; Fujishige, S.; Ando, I. *J. Phys. Chem.* **1990**, *94*, 5154–5158.
(47) Okada, Y.; Tanaka, F. *Macromolecules* **2005**, *38*, 4465–4471.
(48) Ono, Y.; Shikata, T. *J. Am. Chem. Soc.* **2006**, *128*, 10030–10031.
(49) Schild, H. G. *Prog. Polym. Sci.* **1992**, *17*, 163–249.
(50) Wang, X. H.; Qiu, X. P.; Wu, C. *Macromolecules* **1998**, *31*, 2972–2976.
(51) Wu, C.; Zhou, S. Q. *Macromolecules* **1995**, *28*, 8381–8387.
(52) Wu, C.; Zhou, S. Q. *Macromolecules* **1995**, *28*, 5388–5390.
(53) Ciampolini, M. N., N. *Inorg. Chem.* **1966**, *5*, 41–44.
(54) Wu, P.; Feldman, A. K.; Nugent, A. K.; Hawker, C. J.; Scheel, A.; Voit, B.; Pyun, J.; Frechet, J. M. J.; Sharpless, K. B.; Fokin, V. V. *Angew. Chem., Int. Ed.* **2004**, *43*, 3928–3932.
(55) Chen, G. J.; Tao, L.; Mantovani, G.; Ladmiral, V.; Burt, D. P.; Macpherson, J. V.; Haddleton, D. M. *Soft Matter* **2007**, *3*, 732–739.
(56) Pal, M.; Parasuraman, K.; Yeleswarapu, K. R. *Org. Lett.* **2003**, *5*, 349–352.
(57) Lu, F. S.; Xiao, S. Q.; Li, Y. L.; Liu, H. B.; Li, H. M.; Zhuang, J. P.; Liu, Y.; Wang, N.; He, X. R.; Li, X. F.; Gan, L. B.; Zhu, D. B. *Macromolecules* **2004**, *37*, 7444–7450.
(58) Li, C. H.; Ge, Z. S.; Liu, H. W.; Liu, S. Y. *J. Polym. Sci., Part A: Polym. Chem.* **2009**, *47*, 10.1002/pola.23461.
(59) Rostovtsev, V. V.; Green, L. G.; Fokin, V. V.; Sharpless, K. B. *Angew. Chem., Int. Ed.* **2002**, *41*, 2596–2599.
(60) Tornoe, C. W.; Christensen, C.; Meldal, M. *J. Org. Chem.* **2002**, *67*, 3057–3064.
(61) Xia, Y.; Burke, N. A. D.; Stover, H. D. H. *Macromolecules* **2006**, *39*, 2275–2283.
(62) Xia, Y.; Yin, X. C.; Burke, N. A. D.; Stover, H. D. H. *Macromolecules* **2005**, *38*, 5937–5943.
(63) Wu, T.; Zhang, Y. F.; Wang, X. F.; Liu, S. Y. *Chem. Mater.* **2008**, *20*, 101–109.
(64) Jiang, X. Z.; Ge, Z. S.; Xu, J.; Liu, H.; Liu, S. Y. *Biomacromolecules* **2007**, *8*, 3184–3192.
(65) Zhang, J. Y.; Zhou, Y. M.; Zhu, Z. Y.; Ge, Z. S.; Liu, S. Y. *Macromolecules* **2008**, *41*, 1444–1454.
(66) Xu, J.; Ye, J.; Liu, S. Y. *Macromolecules* **2007**, *40*, 9103–9110.
(67) Matyjaszewski, K.; Shipp, D. A.; Wang, J. L.; Grimaud, T.; Patten, T. E. *Macromolecules* **1998**, *31*, 6836–6840.
(68) Ladmiral, V.; Legge, T. M.; Zhao, Y. L.; Perrier, S. *Macromolecules* **2008**, *41*, 6728–6732.
(69) Li, Y.; Yang, J. W.; Benicewicz, B. C. *J. Polym. Sci., Part A: Polym. Chem.* **2007**, *45*, 4300–4308.
(70) Li, G.; Zheng, H. T.; Bai, R. K. *Macromol. Rapid Commun.* **2009**, *30*, 442–447.
(71) Sumerlin, B. S.; Tsarevsky, N. V.; Louche, G.; Lee, R. Y.; Matyjaszewski, K. *Macromolecules* **2005**, *38*, 7540–7545.
(72) Okamura, H.; Ide, N.; Minoda, M.; Komatsu, K.; Fukuda, T. *Macromolecules* **1998**, *31*, 1859–1865.
(73) Chu, C. C.; Wang, L. Y.; Ho, T. I. *Macromol. Rapid Commun.* **2005**, *26*, 1179–1184.
(74) André, X.; Zhang, M. F.; Muller, A. H. E. *Macromol. Rapid Commun.* **2005**, *26*, 558–563.
(75) Arotçaréna, M.; Heise, B.; Ishaya, S.; Laschewsky, A. *J. Am. Chem. Soc.* **2002**, *124*, 3787–3793.
(76) Bo, Q.; Zhao, Y. *J. Polym. Sci., Part A: Polym. Chem.* **2006**, *44*, 1734–1744.
(77) Butun, V.; Armes, S. P.; Billingham, N. C.; Tuzar, Z.; Rankin, A.; Eastoe, J.; Heenan, R. K. *Macromolecules* **2001**, *34*, 1503–1511.
(78) Butun, V.; Billingham, N. C.; Armes, S. P. *J. Am. Chem. Soc.* **1998**, *120*, 11818–11819.
(79) Li, Y. T.; Lokitz, B. S.; Armes, S. P.; McCormick, C. L. *Macromolecules* **2006**, *39*, 2726–2728.
(80) Liu, S. Y.; Armes, S. P. *J. Am. Chem. Soc.* **2001**, *123*, 9910–9911.
(81) Liu, S. Y.; Armes, S. P. *Angew. Chem., Int. Ed.* **2002**, *41*, 1413–1416.
(82) Liu, S. Y.; Armes, S. P. *Langmuir* **2003**, *19*, 4432–4438.
(83) Liu, S. Y.; Billingham, N. C.; Armes, S. P. *Angew. Chem., Int. Ed.* **2001**, *40*, 2328–2331.
(84) Liu, S. Y.; Weaver, J. V. M.; Tang, Y. Q.; Billingham, N. C.; Armes, S. P.; Tribe, K. *Macromolecules* **2002**, *35*, 6121–6131.
(85) Ma, Y. H.; Tang, Y. Q.; Billingham, N. C.; Armes, S. P.; Lewis, A. L.; Lloyd, A. W.; Salvage, J. P. *Macromolecules* **2003**, *36*, 3475–3484.
(86) Mountrichas, G.; Pispas, S. *Macromolecules* **2006**, *39*, 4767–4774.
(87) Munoz-Bonilla, A.; Fernandez-Garcia, M.; Haddleton, D. M. *Soft Matter* **2007**, *3*, 725–731.
(88) Narain, R.; Armes, S. P. *Biomacromolecules* **2003**, *4*, 1746–1758.
(89) Schilli, C. M.; Zhang, M.; Rizzardo, E.; Thang, S. H.; Chong, Y. K.; Edwards, K.; Karlsson, G.; Muller, A. H. E. *Macromolecules* **2004**, *37*, 7861–7866.
(90) Tang, Y. Q.; Liu, S. Y.; Armes, S. P.; Billingham, N. C. *Biomacromolecules* **2003**, *4*, 1636–1645.
(91) Zhang, W.; Shi, L.; Ma, R.; An, Y.; Xu, Y.; Wu, K. *Macromolecules* **2005**, *38*, 8850–8852.
(92) Zhu, Z. Y.; Armes, S. P.; Liu, S. Y. *Macromolecules* **2005**, *38*, 9803–9812.
(93) Topp, M. D. C.; Dijkstra, P. J.; Talsma, H.; Feijen, J. *Macromolecules* **1997**, *30*, 8518–8520.
(94) Virtanen, J.; Holappa, S.; Lemmetyinen, H.; Tenhu, H. *Macromolecules* **2002**, *35*, 4763–4769.
(95) Motokawa, R.; Morishita, K.; Koizumi, S.; Nakahira, T.; Annaka, M. *Macromolecules* **2005**, *38*, 5748–5760.
(96) Zhang, W. Q.; Shi, L. Q.; Wu, K.; An, Y. G. *Macromolecules* **2005**, *38*, 5743–5747.
(97) Yan, J. J.; Ji, W. X.; Chen, E. Q.; Li, Z. C.; Liang, D. H. *Macromolecules* **2008**, *41*, 4908–4913.